

Synthesis of a novel hydroxamic acid flotation collector and its flotation separation of malachite against quartz

Xin Sun ^{1,2}, Lingyun Huang ^{1,2}, Dandan Wu ^{1,2}, Bo Hu ^{1,2}, Mei Zhang ^{1,2}, Yaming Li ^{1,2}, Xiong Tong ²

¹ State Key Laboratory of Complex Nonferrous Metal Resources Clean Utilization, Faculty of Metallurgical and Energy Engineering, Kunming University of Science and Technology, Kunming 650093, China.

² Faculty of Land Resources Engineering, Kunming University of Science and Technology, Kunming 650093, China.

Corresponding author: hly@kust.edu.cn (Lingyun Huang)

Abstract: This paper proposes a promising chelating collector, phenyl propyl hydroxamic acid (BPHA), to directly float malachite for the separation of malachite against quartz. The flotation performance and mechanism was investigated via microflotation tests, as well as through contact angle, Scanning Electron Microscope and Energy Dispersive Spectrometer (SEM-EDS), zeta potential, adsorption capacity, Fourier transform infrared spectroscopy (FT-IR), and X-ray photoelectron spectroscopy (XPS) analyses. The results of microflotation tests showed that BPHA has a strong ability to collect malachite and a significant selectivity against quartz. The contact angle tests showed that BPHA effectively adsorbed onto the mineral surface and could improve the hydrophobicity of the malachite surface. SEM-EDS and adsorption capacity analyses further indicated that BPHA adsorbed onto the surface of malachite. The FT-IR results suggested that BPHA could react with Cu²⁺ ions and facilitate strong chemical adsorption onto the surface of malachite. Furthermore, zeta potential and XPS analyses provided clear evidence that BPHA exhibited a stronger affinity for malachite and a weaker interaction with quartz.

Keywords: flotation, collector, malachite, hydroxamic acid, direct flotation, adsorption

1. Introduction

With the increasing consumption of sulfide copper minerals, copper oxide minerals have gradually been a potential resource for extracting copper metals in importance. As malachite (Cu₂CO₃(OH)₂) is one of the abundant copper oxide minerals, its development and application has attracted further attention (Lee et al., 2009; Xu et al., 2014; Marion et al., 2017; Yu et al., 2021).

Direct flotation is usually applied as an efficient approach for the separation and enrichment of copper oxide ores with flotation reagents, in which collectors react with mineral surfaces modifying hydrophobicity of targeted minerals. The process method of presulfidization flotation had been applied in the commercial for years, which posed many problems (Lee et al., 1998; Kalichini et al., 2017) and as a consequence direct flotation process was in focus extensively. Traditional reagents used in oxide copper ore industrial flotation are xanthate (Huang et al., 2019), fatty acid (Choi et al., 2016), amine (Deng et al., 1991), and chelating collectors (Lu et al., 2021; Huang et al., 2019) etc. Malachite does not respond well to single xanthate collector flotation, as a result, a previous sulphidization was required to change its surface properties similar to that of sulphide counterparts. However, xanthate exhibited poor selectivity to separate malachite from gangue minerals with a low copper recovery, for the floatability of copper oxide minerals was inhibited by the excessive dose of sulfidizing agents. Researchers have strived to modify fatty acid for prompting its flotation power on account of its poor selectivity, although fatty acid collectors have the same functional group -- carboxyl group -- the effects of collectors under different carbon chains and branch chains are obviously different from oxide copper minerals and other calcium-containing gangue minerals, there are still no more breakthroughs about them in recent years. Phosphorus compounds have been investigated for separation malachite against calcite or quartz, due to their strong affinity toward copper oxides surface via its O atoms of P-OH and

P=O (Marcinko et al., 2004; Fonder et al., 2019; Fan et al., 2019; Ai et al., 2021), but they still need sufficient research to achieve industrialization.

Chelating collectors were widely applied in the direct flotation of malachite, especially hydroxamic acids collectors (Yu et al., 2021). Hydroxamic acids have been proved to be available and considered environmentally friendly chelating reagents for the flotation of metal oxide ores (Elizondo-Álvarez et al., 2021). However, hydroxamic acid collectors have shown poor selectivity in the flotation malachite against gangue minerals, it is of a significant problem (Yu and Wang, 2018, Li et al., 2018, Li and Rao, 2019, Mehdilo et al., 2013). Previous research have been conducted improving the performance of the hydroxamic acids through Benzohydroxamic acid (BHA) based structural modification. N-hydroxy-N-benzyl acetamide (NHNBA), N-hydroxy-N-benzyl butyramide (NHNBB), N-hydroxy-N-phenyl acetamide (NHNPA) and N-hydroxy-N-phenyl butyramide (NHNPB) four BHA-based compounds was synthesized as flotation collectors for the first time, which exhibited superior collecting ability and favorable selectivity for the flotation separation of malachite from calcite and quartz compared to that of BHA under pH 8 (Lu et al., 2021). N-hydroxy-N-arylamides exhibited superior collecting ability for malachite, and achieved high selective separation malachite from calcite and quartz, which was modified through the structural of BHA (Marion et al., 2017). Hao et al. (2021) posed a novel X-shaped collector associated with the effect of two hydroxamic acid groups, due to the double branched alkyl chain has enhanced the selectivity. This study indicated that the large steric hindrance and lattice mismatch between collector and minerals impede the interaction of mineral surface, the lattice matching promotes the adsorption of collector on target mineral while rendering the high selectivity of collector in minerals flotation separation system. Li et al. (Li et al., 2019; Xu et al., 2015; Luo et al., 2021) demonstrated the mechanism that N-hydroxy-N-arylamides formed a five-membered-ring complex onto the malachite surfaces by chemisorption through the reactions of the C=O and -NOH groups, which was in accordance with the adsorption mechanism of malachite with the tert-butylsalicylaldehyde. Yu et al. (2021) synthesized cinnamichydroxamic acid (CHA) by adding carbon chain to benzohydroxamic acid and successfully separated malachite against calcite though the chemical adsorption of CHA on malachite surfaces.

Although the structural modification of hydroxamates has been enhanced their performance in mineral flotation, the mechanism between the mineral surfaces and the aqueous hydroxamic acids has limit information on malachite flotation.

Above studies intrigued us further to exploit BHA structural modifications of the hydrophobic groups of -C=NH-OH group for malachite flotation. In this paper, the structure of Benzohydroxamic acid was modified, and phenylpropionichydroxamic acid (BPHA) was synthesized and introduced as a potential malachite collector. The separation performance and adsorption mechanism were explored for malachite flotation through micro-flotation experiments, contact angle, SEM-EDS, Zeta potential, adsorption capacity, Fourier transform infrared spectroscopy (FT-IR), and X-ray Photoelectron Spectroscopy (XPS) analysis. These findings will be helpful to promote the effective separation of quartz from malachite via direct flotation.

2. Materials and methods

2.1. Mineral samples and reagents

Malachite samples were originated from Yunnan province, China. The product of minerals was obtained from raw ore by crushed and manual selection, crushing, grinding, screening. The fractions with particle sizes between 38 μm and 76 μm were gathered for the micro-flotation tests. And the ones with particle size -5 μm were collected and prepared for FT-IR, zeta potential, SEM-EDS, adsorption capacity, and XPS measurements. The X-ray diffraction (XRD) results and chemical analysis of malachite were listed in Fig.1 and Table 1, which showed that the purity of malachite was 97.15%. The quartz was purchased from Xinchuiyuan Co., Ltd with a purity of 98.40%.

The phenyl propyl hydroxamic acid (BPHA) was synthesized in the lab and its purity was over 98.50%, whose synthesis route is listed in Scheme 1. Hydroxylamine hydrochloride and NaOH were stirred in deionized aqueous solution with a mass ratio of 1:2.2 for 30min at 30°C. Subsequently, methyl phenylpropionate and free hydroxylamine solution were put into a three-mouth flask with a molar ratio

of 1:1.2 and reacted at 50°C for 4 hours; After that, the obtained aqueous phase was conditioned to a pH value of 4~5 and separated the oil phase from the water phase with a separating funnel. Methyl Isobutyl Carbinol (MIBC) provided by Aladdin (China) was applied as frother, Analytical grade HCl and NaOH (Sinopharm Chemical Reagent Co., Ltd, China) was employed as pH regulators. The reagents used in the experiment were chemical pure compounds. The water was deionized water. The chemical reaction formula for the synthesis of phenylprooxime acid is shown in scheme (1).

Table 1. X-ray fluorescence spectrum analysis of pure malachite minerals.

Elements	Cu	Al	Zn	P	S	Si	Fe	Mn	Cl	Others
Content(%)	55.83	0.07	0.05	0.04	0.003	0.06	0.01	0.02	0.01	43.91

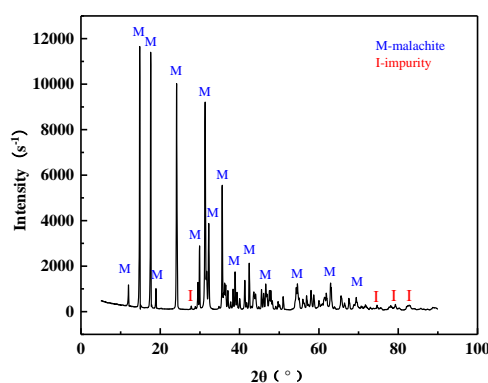
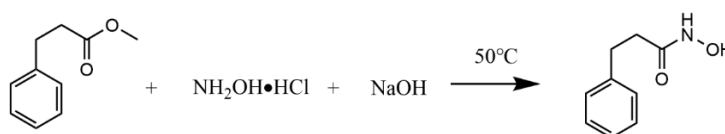


Fig. 1. X-ray diffraction pattern of pure malachite minerals



Scheme 1. Synthetic route of BPHA

2.2. Micro-flotation experiments

Micro-flotation experiments of single mineral and artificially mixed minerals were operated in an XFG-II flotation machine (Jilin, China) with a 40 mL cell at an impeller speed of 1300 r/min. In each test, 2.00g of single minerals were dispersed in 35 mL deionized water in the flotation cell. After regulating the pulp pH for 1 min, the collector (BPHA) and frother (MIBC) were added into the pulp suspension in sequence and then conditioned for 5 min and 1 min, respectively. The conditioned slurry was conducted for 5 min. The froth products and tailings were collected, dried, and weighed, for calculation of mineral recovery. As for artificially mixed minerals, 5.00g of mixed minerals (2.00g of malachite and 3.00g of quartz) were used as the flotation minerals. The dosage of BPHA and slurry pH value were fixed as the optimal value from single mineral flotation experiments. The flotation products were analyzed by XRF and used to calculate the flotation recoveries of malachite and quartz. All flotation tests at least three experiments were recorded, and the average values and standard deviations were calculated with an error of less than $\pm 3.00\%$. The reagents used in the experiment were chemical pure compounds. The water was deionized water.

2.3. Contact angle measurements

The wettability of malachite surface measurements after conditioning with different concentrations of BPHA was conducted by an ES-103HA instrument (Beijing). After wet-polishing, the malachite surface was soaked in the BPHA solution for 20 min. The malachite samples were washed by an ultrasonic cleaner and vacuum drying for contact angle measurements. The average value was presented of three independent measurements.

2.4. SEM-EDS measurements

The scanning electron microscope (SEM) testing instrument was XL30ESEM-TM electron microscope of Philips company in the Netherlands. The energy spectrum analysis adopts the genesis energy spectrometer of the EDAX company. Malachite samples after the action of BPHA agents to be tested were placed in a vacuum drying oven for drying treatment, and a certain amount of samples were taken for SEM-EDS analysis and detection after drying. In this study, SEM and EDS were used to detect the differences in surface morphology and chemical composition of Malachite before and after adsorption by BPHA.

2.5. Zeta potential measurements

Zeta potential values of malachite and quartz samples in the presence and absence of BPHA were carried out by the JS94H electrophoresis instrument. 0.05g of -5 μm samples were put into 40mL of 5×10^{-4} mol/L KCL solutions. After stirring for 5 min, the pH values were conditioned with dilute NaOH or H₂SO₄ solutions. Following, the mixture was agitating and then settled for 5min, respectively. The suspension was collected for the zeta potential measurement. The obtained values were the average of five independent measurements and the standard deviation was calculated.

2.6. FTIR spectrum

FTIR spectra were acquired using an FTIR-740 infrared spectrometer (Thermo Nicolet, USA). Before these measurements, 0.50 g of malachite or quartz particles (< 5 μm in size) were added into a beaker containing an aqueous solution with or without BPHA at a pH of 8. The beaker was subsequently agitated in a thermostat-coupled water bath at 25 °C for 1h. After achieving adsorption equilibrium via agitation, the mineral samples were filtered and rinsed with water three times and subsequently dried until they were completely dehydrated. The resulting samples were used for FTIR analysis with KBr disk pellets in a wavenumber range of 400–4000 cm^{-1} .

2.7. Determination of adsorption capacity

Put 0.50g malachite sample into 100mL beaker and add different concentrations of BPHA solution. After adjusting the suspension to the desired pH value with dilute NaOH or HCl solutions, distilled water was added to make the total volume of 40 mL, and the residual concentration of BPHA was determined by UV-2700 UV-visible spectrophotometer. According to the difference between the original concentration and the residual concentration, the adsorption capacity of BPHA on the given malachite surface was calculated, as shown in Eq. (1).

$$\tau = \frac{(C_0 - C)V}{m} \quad (1)$$

where: τ indicates the adsorption concentration of minerals (mol/g); C_0 indicates the concentration of flotation reagent solution (mol/L); C indicates the concentration of flotation reagent solution (mol/L); V indicates the volume of flotation reagent solution (mL); m indicates the mass of Malachite (g).

2.8. XPS measurements

XPS spectra of malachite and quartz before and after BPHA treatment were collected by Thermo Fisher ESCLAB 250Xi photoelectron spectrometer. The preparation of the mineral sample was consistent with the experimental results of the IR spectrum. During the analysis, the vacuum pressure remained between 10^{-10} and 10^{-9} Torr. The pass energy was 20 eV and the take-off angle was 45°.

3. Results and discussion

3.1. Flotation experiments

3.1.1. Micro-flotation of single minerals

The recoveries of malachite are presented in Fig. 2 with variation of the BPHA dosage and the pulppH. The effect of pH on the flotation recovery of malachite with BPHA is presented in Fig. 2(a) at 100 mg/L BPHA and 40 mg/L MIBC. The effect of BPHA concentration on the flotation recovery of malachite is presented in Fig. 2(b) at pH 8.50 and 40 mg/L MIBC.

Fig. 2(a) shows that the pH value of the solution has a great influence on the enrichment of malachite by BPHA. When the pH value of the solution is strongly acidic and alkaline, the collection performance of BPHA is the worst. When the pH value of the flotation solution is 8, the ability of BPHA to collect malachite is the best and the recovery rate of malachite reached 95.54%, the recovery of quartz is 7.07%. As observed in Fig. 2(b), BPHA dosage has a great influence on the flotation recovery of malachite. The flotation results also demonstrate that the optimal dosage of BPHA for malachite is approximately 60.00mg/L, at which point the recovery of malachite could reach over 95.00%.

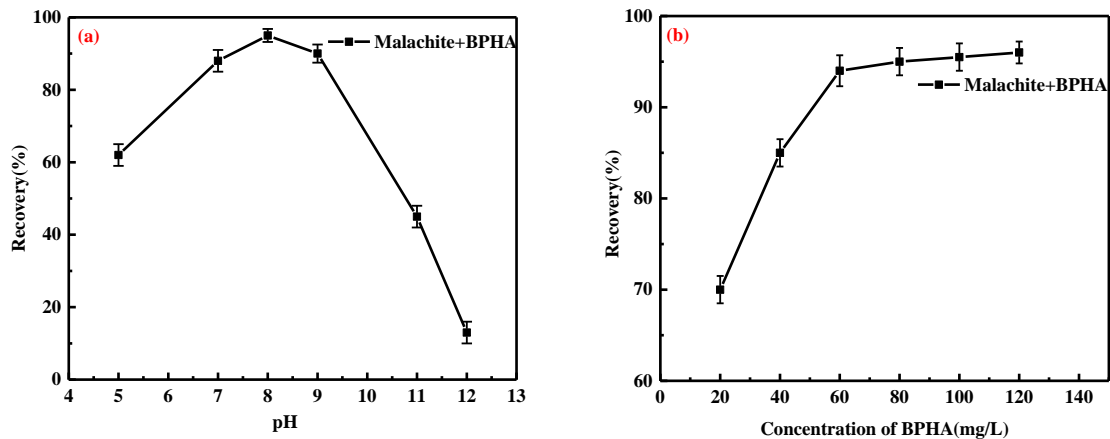


Fig. 2. Flotation recovery of malachite as a function of pH value and concentration of BPHA. (a) The flotation performance of malachite as a function of pH in the presence of 100 mg/L BPHA. (b) The influences of BPHA dosage on the flotation performance of malachite at a pH of approximately 8.)

3.1.2. Flotation of artificial mixed minerals

It is known from the above microflotation results for single minerals that BPHA exhibits a stronger affinity and a superior selectivity for malachite, and BPHA might be regarded as a potential collector to separate malachite from quartz gangue minerals. Therefore, we designed an experiment for the flotation separation of artificially mixed minerals with a malachite to quartz mass ratio of 2 to 3 and investigated its separation efficiency with different pH. The fixed optimum concentration of collector was 60 mg/L for mixed ore test, and the fixed concentration of MIBC was 40 mg/L to test the influence of pH on the separation of malachite and quartz flotation, as shown in Fig. 3.

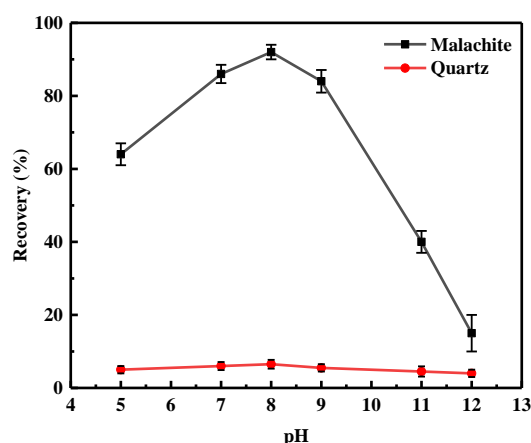


Fig. 3. Flotation performances of malachite and quartz as a function of pH in the presence of 60 mg/L BPHA

As observed in Fig. 3, the flotation results also demonstrate that the optimal pH for malachite is approximately 8, at which point the recovery of malachite could reach over 90.00%, while the recovery of quartz is only approximately 7.00%. This phenomenon indicates that BPHA exhibits a better selectivity for malachite than for quartz. As can be seen from Fig. 3, under the condition of low alkali,

BPHA can separate malachite and quartz well. BPHA is a good collector with good selectivity in low alkali condition.

3.2. Surface wettability studies

Hydrophobicity is an important parameter affecting the mineral collecting ability of a collector, which determines the floatability of mineral particles after their interaction with the collector (Yu et al., 2021). By studying the contact angle, we can see the size of the contact angle before and after the agent acts on malachite, so we can infer whether the agent adsorbs the malachite surface and judge the floatability of malachite. The dosage of the BPHA collector was set at 200.0 mg/L. The results of the contact angle measurements are exhibited in Fig. 4 and Fig. 5.

The untreated malachite contact angle (47.13°) is consistent with the reported value (Lu et al., 2021; Liqing et al., 2019). As shown in Fig. 4, the contact angle of malachite treated with hydroxamic acid increased significantly, from 47.13° to 90.08° , indicating that the surface hydrophobicity of malachite was enhanced. Then, the relationship between the BPHA concentration and malachite surface contact angle was tested. The test results are shown in Fig. 5.

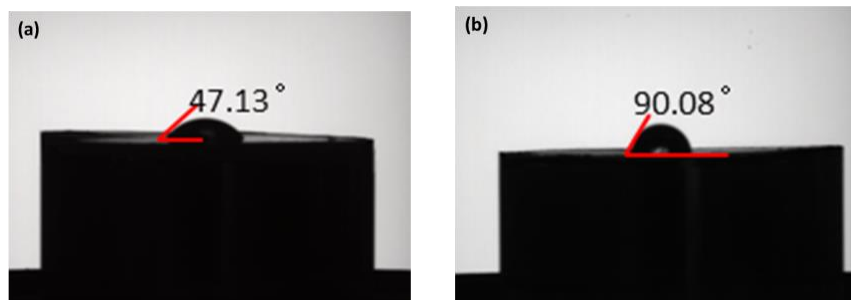


Fig. 4. Surface contact angle of malachite before and after BPHA collector treatment. (a) Surface contact angle of malachite before BPHA collector treatment, (b) Surface contact angle of malachite after BPHA collector treatment)

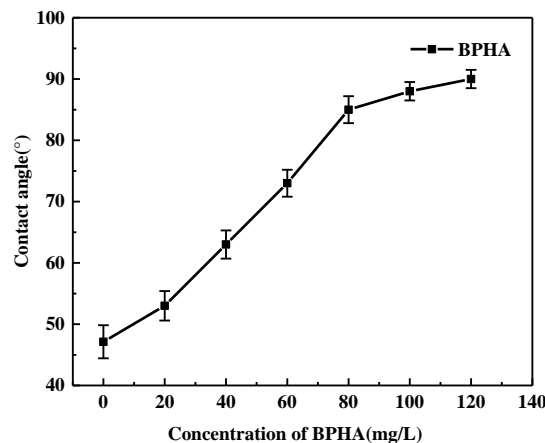


Fig. 5. Influences of BPHA dosage on the contact angle performance of malachite at a pH of approximately 8

As shown in Fig. 5, the mineral surface contact angle increases with increasing reagent dosage. When the concentration of reagent is between 40.00 mg/L and 60.00 mg/L, the mineral surface contact angle rises the fastest. When the concentration is higher than 60.00 mg/L, the mineral surface contact angle tends to be stable, and the final value is approximately 88° . The contact angle test shows that the BPHA collector can adsorb effectively onto the mineral surface and increase the hydrophobicity of the mineral surface.

3.3. SEM-EDS analysis

To determine the changes in malachite surface components after BPHA treatment, SEM-EDS spectra of malachite raw ore and surface after BPHA treatment are shown in Fig. 6.

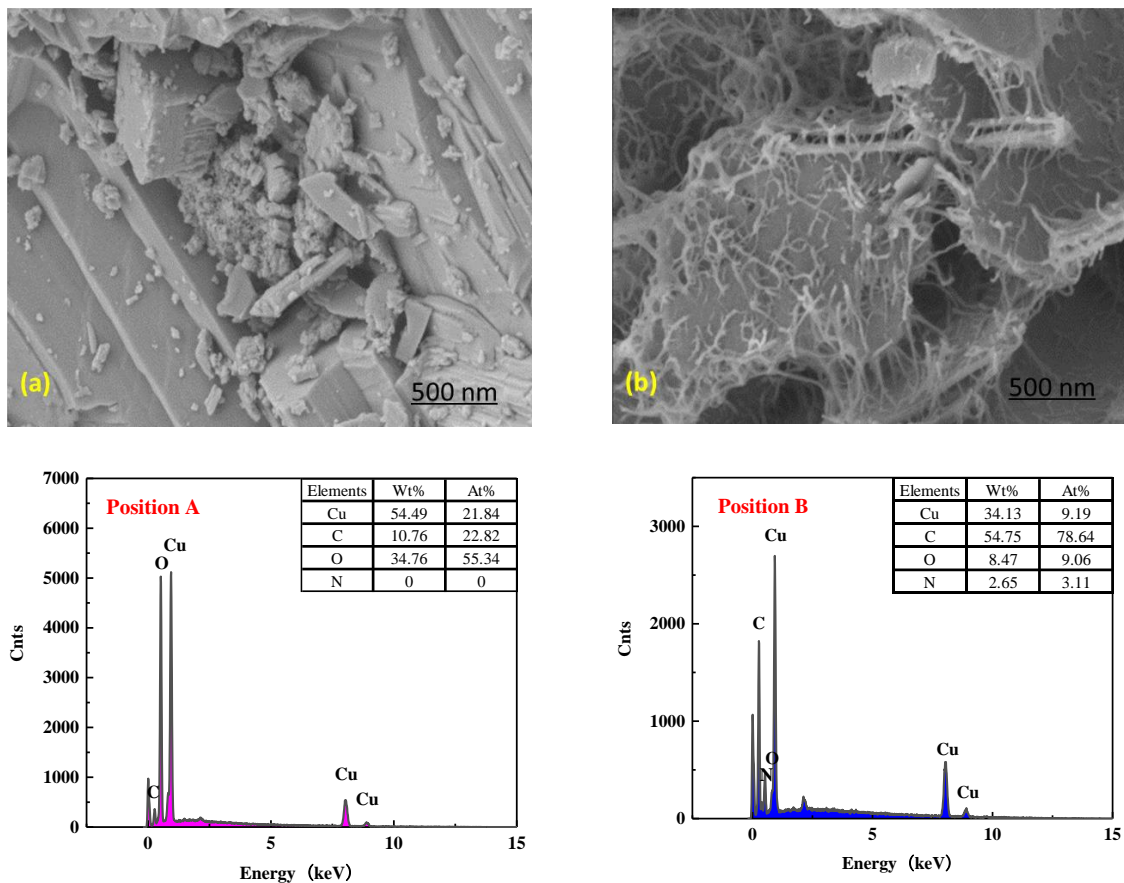


Fig. 6. The SEM images of a mineral surface treated (a) before and (b) after BPHA. (Point A, B, represent EDS of point A, B respectively)

As seen from Fig. 6, the electronic energy spectra of malachite before BPHA treatment show only the peaks of Cu, C and O, and the semiquantitative EDS analysis results show that the Cu content is 54.49%, which is close to the theoretical Cu content of 57.57% in malachite, indicating that there are no other impurity elements around the detection area and that the malachite minerals are relatively pure.

The electronic energy spectra of malachite after BPHA treatment present peaks of C, O and Cu, while the peak of N 1s detected at the same time, and the content of N is 2.65%. The results of semiquantitative analysis show that the concentration of Cu atoms decreased from 54.49% to 34.13%, and the concentration of N atoms increased from 0 to 2.65%. This is apparently due to the adsorption of BPHA onto the surface of malachite, resulting in a decrease in the Cu atom concentration and an increase in the N atom concentration.

3.4. Zeta potential analysis

The change in zeta potential on the mineral surface could indirectly reflect the change in mineral surface properties (Wang et al., 2021). The function of the zeta potential on the malachite and quartz surfaces with regard to the pH values of the slurry before and after the addition of the collector is shown in Fig. 7.

It presents the effects of pH on the zeta potentials of malachite and quartz under BPHA conditions with or without 60.0 mg/L. The isoelectric point (IEP) of malachite was located at pH 8.4, which was similar to other reports (Yu et al., 2021; LU et al., 2021), while quartz had no zero electric point within the whole pH range (Li et al., 2019). With the addition of BPHA, the zeta potential curves of malachite and quartz were negatively shifted over the entire studied pH range. When the BPHA collector is added, malachite has an obvious negative shift within pH 5.0–12.0. Moreover, the malachite has no IEP at pH 5–12. These changes indicate that BPHA has adsorbed onto the malachite surface within pH 5.0–12.0. Moreover, the data for quartz display a negative trend across the pH range investigated in Fig. 7,

as presented in previous literature. Interestingly, there are few apparent shifts occurring for quartz before and after BPHA addition. This phenomenon implies a very small adsorption of BPHA on the quartz surface. Compared with the results of the single mineral flotation test, the pH range that results in a better flotation performance of malachite is approximately pH 7–pH 10, and the dynamic potential on the surface of malachite minerals decreased the most, which is mainly caused by the chemical adsorption of hydroxamic acid anions dissociated by BPHA onto the surfaces of the malachite minerals. Furthermore, the degree of potential migration was caused by a large amount of BPHA adsorbed onto the surface of malachite, which is consistent with the semiquantitative trend of the Cu and N elements in the SEM-EDS results.

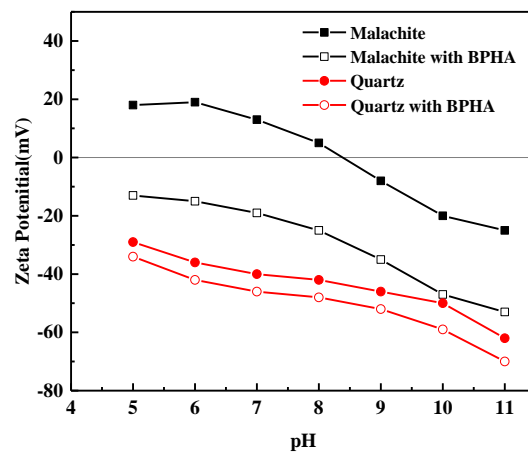


Fig. 7. Zeta potentials of malachite and quartz with or without 60 mg/L BPHA

3.5. FT-IR spectra analysis

The infrared spectra collected before and after the action of malachite and BPHA are shown in Fig. 8. The mechanism of action of the BPHA collector on the surface of malachite ore is studied through infrared spectrum analysis.

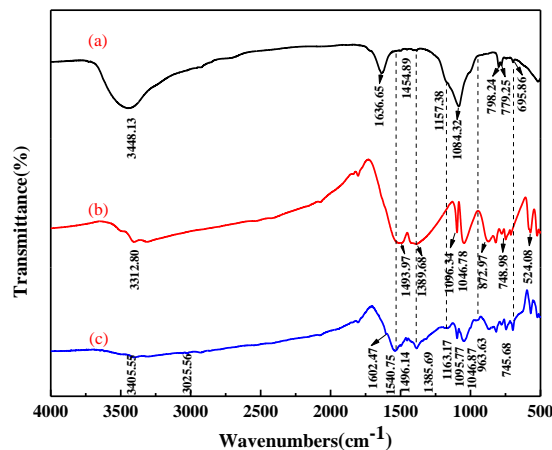


Fig. 8. IR spectra of (a) BPHA, (b) malachite and (c) malachite after BPHA absorption

Fig. 8a shows the infrared spectrum of BPHA, and 3448.13 cm^{-1} is the superposition of the stretching vibration peaks of O-H and N-H. The stretching vibration peak of C-H on the aromatic ring is at 3026.64 cm^{-1} , and the stretching vibration absorption peak of C=O is at 1636.65 cm^{-1} . The peak at 1084.32 cm^{-1} is the superposition of the stretching vibration peaks of C-N and N-O (Yin et al., 2019). Fig. 8b shows the infrared spectrum of malachite, including the stretching vibration peak of -OH at 3312.80 cm^{-1} and the bending vibration absorption peak of -OH at 1046.94 cm^{-1} (Wang et al., 2021). The symmetrical stretching vibration peak of CO_3^{2-} was observed at 1096.34 cm^{-1} , and the asymmetric stretching vibration peaks of CO_3^{2-} were observed at 1493.97 cm^{-1} and 1389.68 cm^{-1} . The peaks at 872.97 , 748.98 and 524.08 cm^{-1} are

characteristic absorption peaks of CO_3^{2-} (Wang et al., 2021). Fig. 8c is the infrared spectrum after the action of malachite ore and BPHA; new peaks appear at 1602.47 cm^{-1} , 1540.75 cm^{-1} , 1163.17 cm^{-1} and 745.68 cm^{-1} . The peak at 1602.47 cm^{-1} is the stretching vibration of C=O, the peak at 1540.75 cm^{-1} (Lenormand et al., 1979) is the characteristic absorption of copper hydroxamic acid, the peak at 1163.17 cm^{-1} is the stretching vibration of C-N, the peak at 745.68 cm^{-1} is the characteristic absorption of Cu-O, and the C-H stretching vibration of the aromatic ring appears at 3025.56 cm^{-1} . The peaks of C=O and C-N appear in the IR spectra of the surface of malachite. The changes in the IR spectra of the malachite surface indicate that the chemical structure of BPHA may have broken and formed new substances with malachite. Due to the influence of the BPHA hydroxamic group characteristic peak shown in Fig. 8a, the BPHA collector changed the surface properties of malachite ore, causing the characteristic peak of the malachite ore to shift and generate a new peak. The adsorption type of the BPHA collector on the surface of malachite ore was chemical adsorption.

3.6. Adsorption measurement results

To study the interaction between BPHA and malachite, the adsorption capacity of BPHA onto the malachite surface was measured by UV-VIS spectroscopy. The adsorption capacity is shown in Fig. 9. It shows the change in the adsorption capacity of BPHA on the mineral surface with BPHA concentration. With increasing BPHA concentration, the adsorption capacity of BPHA onto malachite increased significantly. The adsorption capacity of malachite remained stable at approximately 2.87 mg/g . From the adsorption capacity results, it can be seen that BPHA has a strong adsorption effect on malachite.

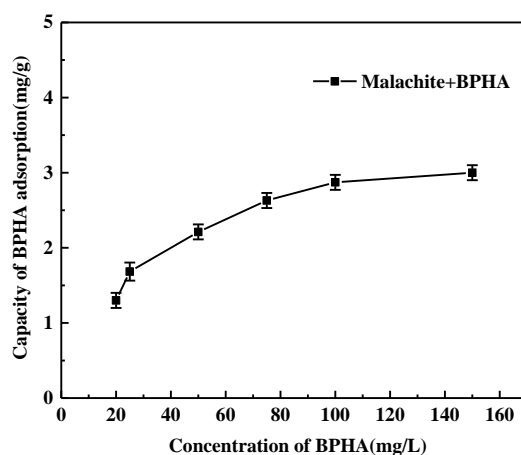


Fig. 9. Influences of BPHA dosage on the adsorption capacity of BPHA onto malachite at a pH of 8, approximately

3.7. XPS analysis

The XPS analysis of malachite before and after BPHA treatment is displayed in Fig. 10. The element content of the XPS spectrum is shown in Table 2.

To determine the chemisorption mechanism of BPHA on malachite surfaces, XPS analyses of malachite particles before and after BPHA treatment were conducted. As displayed in Table 2 and Fig. 10, a new peak at 400 eV (Yu et al., 2021) appeared in the XPS spectrum of malachite after treatment with BPHA, which belongs to N1s (Lu et al., 2021). Table 2 also shows that the malachite surface does

Table 2. Atomic concentrations of the elements in malachite before and after treatment with BPHA.

Species	Atomic concentration/%			
	C1s	N1s	O1s	Cu2p
malachite	33.37	0.00	52.67	13.96
malachite+BPHA	71.47	7.66	16.77	4.10

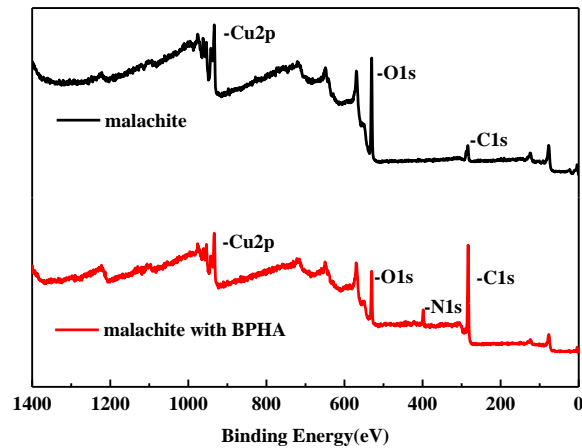


Fig. 10. XPS scan results of the malachite surface before and after treatment with BPHA

not contain N. After the action of BPHA, the malachite surface contains N, and the content of N increases from 0.00% to 7.66%. The content of C1s on the malachite surface increased from 33.37% to 71.47%, the content of Cu2p decreased from 13.96% to 4.10%, and the content of O1s decreased from 52.67% to 16.77%. The contents of carbon and nitrogen increased significantly, whereas those of copper and oxygen showed an evident decline, indicating the adsorption of BPHA onto the malachite surface. The profiles in Fig. 11 indicate that no significant N1s XPS band could be detected for the surface of untreated malachite. However, the N1s band appeared upon BPHA treatment and at 398.26 eV; this peak was attributed to BPHA. This result provides further evidence regarding the adsorption of BPHA onto the malachite surface.

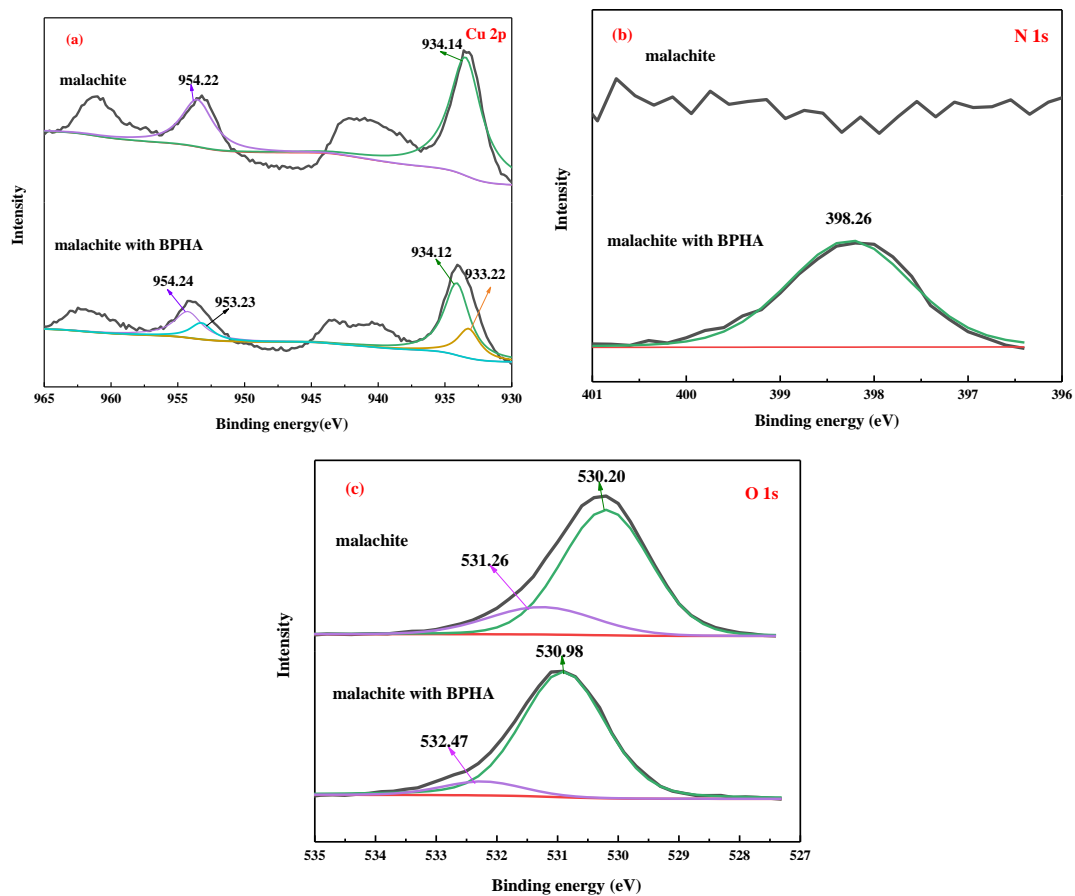


Fig. 11. High-resolution XPS spectra of Cu 2p, N 1s and O 1s of malachite and BPHA-treated malachite. ((a) High-resolution XPS of Cu 2p; (b) High-resolution XPS of N 1s; (c) High-resolution XPS of O 1s)

The Cu 2p XPS profiles show the Cu 2p XPS bands of untreated malachite, which appeared at approximately 934.14 eV and 954.22 eV; these bands were attributed to Cu 2p_{3/2} and Cu 2p_{1/2} in malachite, respectively (Zhang et al., 2020). After treatment with BPHA, the Cu 2p bands split into two peaks, while new peaks appeared at 933.22 eV and 953.23 eV, with no obvious changes in the binding energies of the original peaks. These results indicate that the electronic environment of the copper atoms in malachite was significantly altered after treatment with BPHA; thus, copper atoms presumably act as the active sites of malachite in its interactions with BPHA.

The O1s XPS profile of malachite consists of peaks at approximately 530.2 and 531.26 eV, which were attributed to the oxygen of the carbonate or hydroxyl group in malachite (Feng et al., 2017). After treatment with BPHA, the binding energies of the O1s signals at 530.2 and 531.26 eV shift slightly to 530.98 and 532.47 eV, respectively, indicating that BPHA may react with the copper present on the malachite surfaces to form an adsorbed Cu-BPHA complex (Fang et al., 2020), resulting in a change in the O1s electron cloud density.

According to the above mechanism testing, it is concluded that the malachite BPHA adsorption model is as shown in Fig. 12.



Fig. 12. Adsorption model of BPHA onto the surface of malachite

4. Conclusions

In this paper, a new surfactant, phenylpropyl hydroxamic acid (BPHA), was introduced as a collector for malachite. The flotation performance of malachite and the separation mechanism between malachite and BPHA were explored and evaluated by using microflotation experiments and contact angle, SEM-EDS, zeta potential, adsorption capacity, Fourier transform infrared spectroscopy (FT-IR) and X-ray photoelectron spectroscopy (XPS) analyses.

The results of the microflotation test showed that the best flotation pH of BPHA is pH 8, the best flotation reagent dosage is 60 mg/L, and the best flotation recovery of malachite is 95.00%. The contact angle analysis suggested that the hydrophobicity of malachite increased greatly after BPHA treatment. The surface contact angle of malachite treated with BPHA increased from 47.13° to 90.08°. SEM-EDS and adsorption capacity tests confirmed that BPHA is adsorbed onto the surface of malachite. The infrared spectra show that BPHA could react with Cu²⁺ ions and facilitate strong chemical adsorption onto the surface of malachite. The adsorption model of BPHA on the surface of malachite is shown in Fig. 12. On the other hand, the zeta potential and XPS analysis results provide enough evidence that BPHA possesses a stronger affinity for malachite than quartz and can effectively separate malachite and quartz.

Acknowledgments

The authors acknowledge the support of the National Natural Science Foundation of China (Grant Nos. 51964024, 51904214, and 51804238) and the Foundation of Academic and Technical Talent Cultivation Project of Yunnan Province (Grant No. KKS201952020), the Open Foundation of State Key Laboratory of Complex Nonferrous Metal Resources Clean Utilization (2017).

References

AI, G., HUANG, K. 2021. *Exploration of amino trimethylene phosphonic acid to eliminate the adverse effect of seawater in molybdenite flotation*. International Journal of Mining Science and Technology, 31, 1121-1134

- CHOI, J., CHOI, S.Q., Park K. 2016. *Flotation Behaviour of Malachite in Mono- and Divalent Salt Solutions Using Sodium Oleate as a Collector*. International Journal of Mineral Processing, 146,38–45
- DENG, T., CHEN, J. 1991. *Treatment of Oxidised Copper Ores with Emphasis on Refractory ores*. Mineral Processing and Extractive Metallurgy Review, 7,3–4
- FAN, H., QIN, J., LIU, J. 2019. *Investigation into the Flotation of Malachite, Calcite and Quartz with Three Phosphate Surfactants*. Journal of Materials Research and Technology, 8,5140-5148
- FENG, Q., ZHAO, W., WEN, S. 2017. *Copper Sulfide Species formed on Malachite Surfaces in Relation to Flotation*. Journal of Industrial and Engineering Chemistry, 48,125–132
- FONDER, G., MINET, I. 2011. *Anchoring of Alkylphosphonic Derivatives Molecules on Copper Oxide Surfaces*. Applied Surface Science, 257,6300-6307
- HAIFENG, X., HONG, Z. 2014. *Synthesis of 2-ethyl-2-hexenal Oxime and its Flotation Performance for Copper Ore*. Minerals Engineering, 66, 173-180
- HAO, D., WLA B. 2021. *Selective adsorption of a novel X-shaped surfactant dioctyl di-hydroxamic acid on fluorite surface leading the effective flotation separation of fluorite from calcite and barite*. Journal of Molecular Liquids, 344, 117941
- HUANG, Z.Q., CHENG, C. 2019. *Utilization of a New Gemini Surfactant as the Collector for the Reverse froth Flotation of Phosphate Ore in Sustainable Production of Phosphate Fertilizer*. Journal of Cleaner Production, 221,108–112
- HUANG, Z.Q., CHENG, C. 2019. *Highly Efficient Potassium Fertilizer Production by Using a gemini Surfactant*. Green Chemistry, 21,1406–1411
- KALICHINI M. 2017. *The Role of Pulp Potential and the Sulphidization Technique in the Recovery of Sulphide and Oxide Copper Minerals from a Complex Ore*. Journal of the Southern African Institute of Mining and Metallurgy, 117, 803-810
- LEE, K., ARCHIBALD, D., MCLEAN, J. 2009. *Flotation of Mixed Copper Oxide and Sulphide Minerals with Xanthate and Hydroxamate Collectors*. Minerals Engineering, 22, 395-401
- LEE, J.S., NAGARAJ, D.R., COE, J.E. 1998. *Practical Aspects of Oxide Copper Recovery with Alkyl Hydroxamates*. Minerals Engineering, 11, 929–939
- LENORMAND, J., SALMAN, T. 1979. *Yoon R.H. Hydroxamate Flotation of Malachite*. Canadian Metallurgical Quarterly, 18,125-129
- LI, F., ZHOU, X. 2020. *A Novel Decyl-salicylhydroxamic Acid Flotation Collector: Its Synthesis and Flotation Separation of Malachite Against Quartz*. Powder Technology, 374,522–526
- LI, H., LIU M, LIU Q. 2018. *The effect of non-polar oil on fine hematite flocculation and flotation using sodium oleate or hydroxamic acids as a collector*. Minerals Engineering, 119, 105-115
- LI, Z., RAO F., GUO B. 2019. *Effects of calcium ions on malachite flotation with octylhydroxamate*. Minerals Engineering, 141, 105854
- LI, LQ., ZHAO, JH. 2019. *Flotation Performance and Adsorption Mechanism of Malachite with Tert-butylsalicylaldoxime*. Separation and Purification Technology, 210,843-849
- LI, L., ZHAO, J., XIAO, Y. 2019. *Flotation Performance and Adsorption Mechanism of Malachite with Tert-butylsalicylaldoxime*. Separation and Purification Technology, 210,843-849
- LIU, C., ZHU, Y. 2021. *Studies of benzyl hydroxamic acid/calcium lignosulphonate addition order in the flotation separation of smithsonite from calcite*. International Journal of Mining Science and Technology, 31, 1153-1158
- LU, Y., WU, K., WANG, S. 2021. *Structural Modification of Hydroxamic Acid Collectors to Enhance the Flotation Performance of Malachite and Associated Mechanism*. Journal of Molecular Liquids, 344, 117959
- LUO, L., WU, H., XU, L. 2021. *An in situ ATR-FTIR Study of Mixed Collectors BHA/DDA Adsorption in Ilmenite-titanaugite Flotation System*. International Journal of Mining Science and Technology, 31, 689-697
- MARCINKO, S., FADEEV, A. 2004. *Hydrolytic stability of organic monolayers supported on TiO₂ and ZrO₂*. Langmuir the Acs Journal of Surfaces & Colloids, 20, 2270
- MARION, C., JORDENS, A., LI, R. 2017. *An Evaluation of Hydroxamate Collectors for Malachite Flotation*. Separation & Purification Technology, 183,258-269
- MARTHA ARACELI ELIZONDO-ÁLVAREZ., ALEJANDRO URIBE-SALAS, SIMON BELLO-TEODORO. 2021. *Chemical stability of xanthates, dithiophosphinates and hydroxamic acids in aqueous solutions and their environmental implications*. Ecotoxicology and Environmental Safety, 207, 111509
- REZAI B. 2013. *Effect of chemical composition and crystal chemistry on the zeta potential of ilmenite*. Colloids and Surfaces A: Physicochemical and Engineering Aspects, 428, 111-119

- WANG, H., WEN, S., HAN, G. 2021. *Modification of Malachite Surfaces with Lead Ions and its Contribution to the Sulfidization Flotation*. Applied Surface Science, 550,149-157
- WANG, H., WEN, S., HAN, G. 2021. *Adsorption Characteristics of Pb(II) Species on the Sulfidized Malachite Surface and its Response to Flotation*. Separation and Purification Technology, 264,118-126
- XU, H., ZHONG, H., TANG Q. 2015. *A Novel Collector 2-ethyl-2-hydroxyacetic Hydroxamic acid: Flotation Performance and Adsorption Mechanism to Ilmenite*. Applied Surface Science, 353, 882-889
- YIN, W., SUN, Q., DONG, L. 2019. *Mechanism and Application on Sulphidizing Flotation of Copper Oxide with Combined Collectors*. Transactions of Nonferrous Metals of Society of China, 29, 178–185
- YU, X., WANG L, LIU C. 2018. *Utilization of benzyl aminopropyl dimethoxymethylsilane as collector for the reverse flotation of silicate minerals from magnetite*. Minerals Engineering, 129, 106-111
- YU, X., ZHANG, R., ZENG, Y. 2021. *The Effect and Mechanism of Cinnamic Hydroxamic Acid as a Collector in Flotation Separation of Malachite and Calcite*. Minerals Engineering, 164,106847
- ZHANG, Q., WANG, Y., FENG, Q., Wen, S. 2020. *Identification of Sulfidization Products formed on Azurite Surfaces and its Correlations with Xanthate Adsorption and Flotation*. Applied Surface Science, 511,145594